

CANCER

Epigenetic therapy overcomes treatment resistance in T cell prolymphocytic leukemia

Zainul S. Hasanali,¹ Bikramajit Singh Saroya,² August Stuart,³ Sara Shimko,³ Juanita Evans,⁴ Mithun Vinod Shah,⁵ Kamal Sharma,⁶ Violetta V. Leshchenko,⁷ Samir Parekh,⁷ Thomas P. Loughran Jr.,^{8*} Elliot M. Epner^{9*}

T cell prolymphocytic leukemia (T-PLL) is a rare, mature T cell neoplasm with distinct features and an aggressive clinical course. Early relapse and short overall survival are commonplace. Use of the monoclonal anti-CD52 antibody alemtuzumab has improved the rate of complete remission and duration of response to more than 50% and between 6 and 12 months, respectively. Despite this advance, without an allogeneic transplant, resistant relapse is inevitable. We report seven complete and one partial remission in eight patients receiving alemtuzumab and cladribine with or without a histone deacetylase inhibitor. These data show that administration of epigenetic agents can overcome alemtuzumab resistance. We also report epigenetically induced expression of the surface receptor protein CD30 in T-PLL. Subsequent treatment with the anti-CD30 antibody–drug conjugate brentuximab vedotin overcame organ-specific (skin) resistance to alemtuzumab. Our findings demonstrate activity of combination epigenetic and immunotherapy in the incurable illness T-PLL, particularly in the setting of previous alemtuzumab therapy.

INTRODUCTION

Prolymphocytic leukemia is a rare, aggressive disease comprising 2% of mature lymphoid neoplasms. T cell variant [T cell prolymphocytic leukemia (T-PLL)] is responsible for about 20% of the cases (1). Median age of onset is between 65 and 70 years, and there is a male predilection (2). Common presenting signs include splenomegaly (73%), lymphadenopathy (53%), hepatomegaly (40%), skin manifestations (27%), pleural effusions (12%), and high leukocyte count ($>100 \times 10^9$ cells per liter in 75%). T-PLL cells usually express CD2, CD5, and CD7 and are terminal deoxynucleotidyl transferase–negative (TdT⁻). Most cases also have a CD4⁺/CD8⁻ (65%) phenotype, though CD4⁻/CD8⁺ (13%) and CD4⁺/CD8⁺ (21%) variants exist. Analysis of the peripheral blood shows characteristic prolymphocyte morphology with basophilic cytoplasm, a single nucleolus, and surface protrusions (2, 3). Human T lymphotropic virus 1 (HTLV-1) must be negative by both serology and polymerase chain reaction (PCR) (4).

T-PLL is considered incurable, and treatment is difficult (5). CHOP (cyclophosphamide, vincristine, doxorubicin, prednisone) and single-agent 2'-deoxycoformycin (DCF), cladribine, and fludarabine have shown little success (3, 6, 7). CD52 is highly expressed on all normal lymphocytes, as well as T-PLL cells, providing the rationale for use of alemtuzumab, an anti-CD52 monoclonal antibody, in T-PLL (8). Although approved for B cell chronic lymphocytic leukemia (B-CLL), single-agent alemtuzumab has become the first-line therapy for T-PLL, with higher response rates

than previous regimens (9). The mechanism of action of alemtuzumab and other monoclonal antibodies remains poorly characterized. Antibody-dependent cell-mediated cytotoxicity (ADCC), complement-mediated cytotoxicity (CMC), and direct antitumor effects have been proposed. However, alemtuzumab alone is not a curative approach for T-PLL due to resistance (5).

Aberrant activation and deactivation of transcription through epigenetic changes are associated with tumorigenesis (10, 11). Two changes instrumental in gene silencing are methylation of DNA and acetylation of histone tail lysine residues. The purine analog cladribine has mechanisms of action that make it useful as an epigenetic agent. Cladribine inhibits *S*-adenosyl-*L*-homocysteine hydrolase through inhibition of donation of methyl groups by *S*-adenosyl methionine (7, 12, 13). Vorinostat and romidepsin are both inhibitors of pan–histone deacetylase (HDAC) enzymes and are both approved for treatment of cutaneous T cell lymphoma (CTCL) and peripheral T cell lymphoma. There are many other HDAC inhibitor (HDACi) compounds in development as well (14). Thus, the combination of HDACis with hypomethylating agents such as cladribine is potentially synergistic. Administration of HDACi subsequent to DNA methyltransferase inhibitors synergistically increases expression of silenced tumor suppressors and promotes cell death (15). The ability of cladribine to inhibit both DNA and histone methylation may be critical to the success of this combination therapy.

CD30 (*TNFRSF8*) is a 130-kD membrane glycoprotein receptor, originally identified on Reed-Sternberg cells of Hodgkin's lymphoma (HL). As a member of the tumor necrosis factor receptor (TNFR) superfamily, it is preferentially expressed in developing and activated lymphocytes (16–20) as well as in many cancers, including HL, CTCL, anaplastic large cell lymphoma (ALCL), and mastocytosis (21–23). Members of the TNFR superfamily are classically associated with transducing death signals, but CD30 does not contain the death domain of other TNFRs (24). Regardless of its normal function, CD30 is a target for delivery of potent chemotherapeutics such as brentuximab vedotin.

Brentuximab vedotin is an antibody–drug conjugate consisting of three components: a chimeric immunoglobulin G1 specific for CD30,

¹Department of Microbiology and Immunology, Pennsylvania State University College of Medicine and Penn State Hershey Cancer Institute, Hershey, PA 17033, USA. ²Department of Pathology, St. George's University, True Blue, Grenada. ³Department of Medicine/Hematology-Oncology, Pennsylvania State University College of Medicine and Penn State Hershey Cancer Institute, Hershey, PA 17033, USA. ⁴Department of Anatomic Pathology, Pennsylvania State University College of Medicine, Hershey, PA 17033, USA. ⁵Division of Hematology and Department of Medical Oncology, Mayo Clinic, Rochester, MN 55905, USA. ⁶Shaner Cancer Center Mount Nittany Medical Center/Pennsylvania State University, State College, PA 6803, USA. ⁷Division of Hematology and Medical Oncology, Icahn School of Medicine at Mount Sinai, New York, NY 10029, USA. ⁸Department of Medicine/Hematology-Oncology, UVA Cancer Center, Charlottesville, VA 22903, USA. ⁹Department of Hematology/Oncology, New Mexico VA Health Care System, Albuquerque, NM 87108, USA.

*Corresponding author. E-mail: tploughran@virginia.edu (T.P.L.); epner5@msn.com (E.M.E.)

a microtubule-disrupting agent (auristatin E), and a protease cleavable covalent linker (25, 26). It binds CD30 on the cell surface. When the drug is internalized, the linker is cleaved in the lysosome, releasing auristatin E into the cell. As a targeted therapy, it is currently approved for third- and second-line treatment of HL and ALCL, respectively (27).

We present a case series of eight T-PLL patients who were treated with cladribine, vorinostat/romidepsin/valproic acid, and alemtuzumab. We report overcoming alemtuzumab resistance with these epigenetic drugs in T-PLL. Protein and transcriptional analyses showed that such therapy can activate expression of CD30 in T-PLL cells. This increase in CD30 allows for successful treatment with brentuximab vedotin.

RESULTS

Patient response and outcomes

Patients were predominantly male and aged between 57 and 77 years. They all met the diagnostic criteria of T-PLL. Clinicopathologic features at presentation are summarized in table S1. Patient responses to combined epigenetic and immunotherapy are summarized in Table 1. Full case descriptions of each patient are in the Supplementary Materials. We treated eight patients with both cladribine and alemtuzumab in combination, and seven achieved CR. The rationale for adding cladribine was based on published data and a recently completed phase 2 trial demonstrating synergistic effects between cladribine, vorinostat,

Table 1. Summary of patient treatment response. Disease status, previous treatments, treatment administered, extent of clinical and molecular remission, duration of response, overall survival, and expected survival were tabulated. Survival times are calculated from first treat-

ment with alemtuzumab. Mean time between relapses was 6 months. CR, complete remission; PR, partial response (decrease in white blood cell counts); CNS, central nervous system; Allo, allogeneic; N/A, not applicable.

Patient	Disease status before epigenetic therapy	Previous treatment	Treatment administered	Clinical remission	Molecular remission	Duration of response	Overall survival time	Expected survival*
1	First relapse	CVP (cyclophosphamide, vincristine, prednisone)	Alemtuzumab, cladribine	CR	Yes	16 months	34.3 months	4 months
	Second relapse	Alemtuzumab, cladribine	Alemtuzumab, cladribine	PR	N/A	11.6 months		
	Third relapse	Alemtuzumab, cladribine	Alemtuzumab, brentuximab vedotin	PR	N/A	6.7 months to death, persistent disease		
2	First relapse	Alemtuzumab (6 months CR)	Alemtuzumab, cladribine, vorinostat	CR	Yes	5.3 months	17 months	7.5 – 10 months
	Second relapse	Alemtuzumab, cladribine, vorinostat	Alemtuzumab, cladribine, vorinostat	PR	N/A	2 months		
	Third relapse	Alemtuzumab, cladribine, vorinostat	Alemtuzumab, cladribine, vorinostat	PR	N/A	3.7 months to death, persistent disease		
3	Initial presentation	N/A	Alemtuzumab, cladribine	PR	N/A	5.7 months	5.7 months	20 months
4	Initial presentation	N/A	Alemtuzumab, cladribine	CR	Yes	13.3 months	14.8 months	20 months
	First relapse	Alemtuzumab, cladribine	Alemtuzumab, cladribine	PR	N/A	1.5 months to death, persistent disease, CNS hemorrhage		
5	Initial presentation	N/A	Alemtuzumab, cladribine, vorinostat	CR	Yes	6.3 months	15.3 months	20 months
	First relapse with skin involvement	Alemtuzumab, cladribine, vorinostat	Alemtuzumab, cladribine, romidepsin	PR	N/A	4 months—blood		
	Second relapse with skin involvement	Alemtuzumab, cladribine, romidepsin	Brentuximab vedotin	PR	N/A	5 months to Allo transplant, death, persistent disease		
6	Initial presentation	N/A	Alemtuzumab, cladribine	CR	Yes	0.8 months to Allo transplant	0.8+ months	N/A
7	First relapse	Alemtuzumab (0.3 months)	Alemtuzumab, cladribine, valproic acid	CR	Yes	12 months to Allo transplant referral	12+ months	4 months
8	First relapse	Alemtuzumab (16 months)	Alemtuzumab, cladribine	CR	Yes	6.7 months	23.7+ months	7.5 – 10 months
	Second relapse	Alemtuzumab, cladribine	Alemtuzumab, cladribine	CR	Yes	1+ month		

*Expected survival without transplant (5).

and the monoclonal antibody rituximab in the aggressive B cell malignancy mantle cell lymphoma (MCL) (28–30). Additionally, in vivo studies of B-CLL and breast cancer and in vitro study of MCL cell lines support the ability of cladribine to be both a DNA and histone methylation inhibitor (fig. S1) (7, 31). A full description and diagram of the treatment schedule is presented in Fig. 1. Patient 1 presented with high white blood cell count, anemia, and thrombocytopenia,

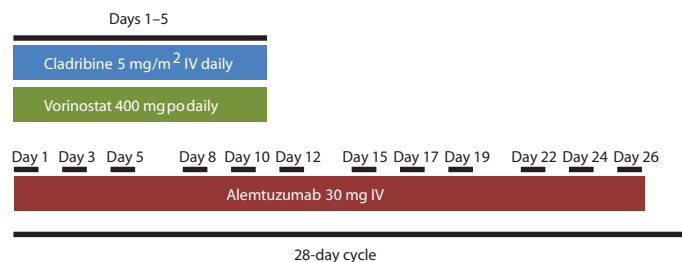


Fig. 1. One cycle of epigenetic therapy consisted of a three-drug combination over 28 days. Patients received cladribine at 5 mg/m² intravenously (IV) each day on days 1 to 5. Those treated with vorinostat were given 400 mg orally (po) each day on days 1 to 5 as well. Patients received 30 mg of alemtuzumab intravenously or subcutaneously once a day on days 1, 3, 5, 8, 10, 12, 15, 17, 19, 22, 24, and 26. One treatment cycle was 28 days. All patients were treated with alemtuzumab and cladribine. Those whose white blood cell counts did not respond well after relapse were also treated with vorinostat. Status of clinical and molecular remissions was evaluated after two to three cycles.

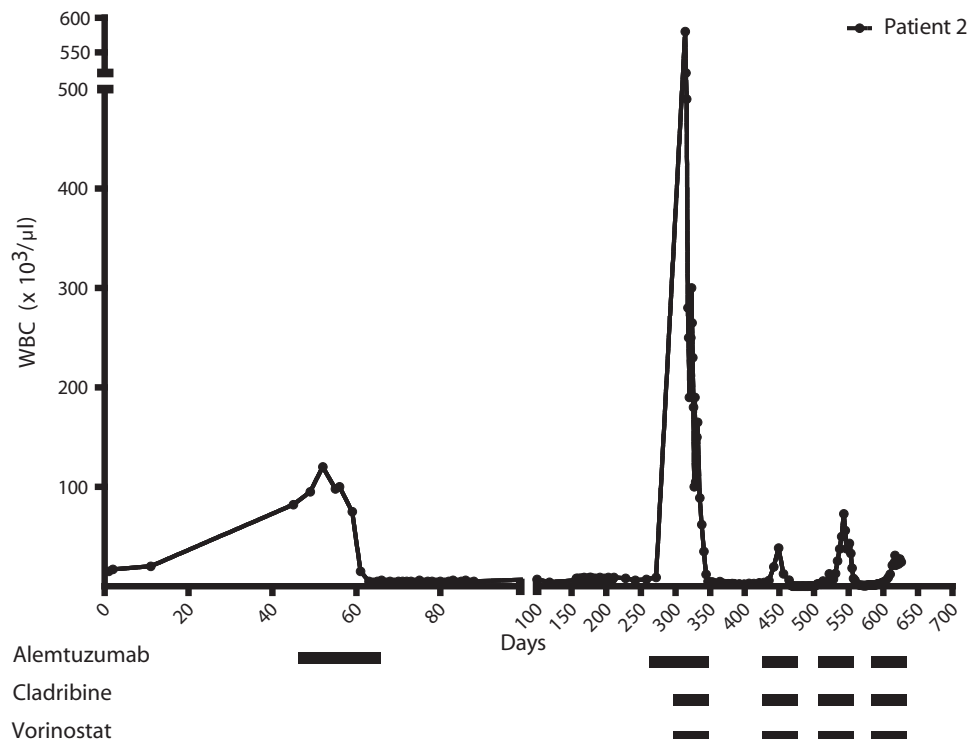


Fig. 2. Epigenetic therapy decreased leukemic white blood cell counts despite multiple relapses. Patient 2's white blood cell (WBC) counts were monitored during treatment. Day 0 was the initial white blood cell count at presentation. The bars beneath the graph represent treatment received by the patient over the corresponding time periods. Graphs for all treated patients are available in fig. S3.

and was first treated with IV alemtuzumab alone. White blood cell count dropped briefly but then continued to rise while on treatment. Cladribine was added, and she achieved CR. She remained in CR for more than 1 year, relapsed, and again achieved CR with cladribine and alemtuzumab. In contrast to the primary refractory pattern of patient 1, patient 2 was representative of the relapse, retreatment pattern. He presented with alemtuzumab-resistant relapse but went into remission after the addition of cladribine and vorinostat. Although he relapsed several times, his disease remained susceptible to treatment with alemtuzumab, cladribine, and vorinostat (Fig. 2). An attempt to identify the cell death mechanism relevant to the combination therapy showed a lack of apoptotic cells despite the rapid decrease in cell count in patients 2 and 3 (figs. S2 and S3). Patients 3, 4, 5, 6, and 8 were treated with combination cladribine and alemtuzumab with or without vorinostat as well. With the exception of patient 3, who achieved PR, these patients also achieved CRs; subsequent relapses remained susceptible to treatment (fig. S3). Patient 7 was treated with cladribine and alemtuzumab but only achieved CR when valproic acid was added. Like vorinostat, valproic acid has HDACi properties (32). It was used, because vorinostat and romidepsin were not available as a result of insurance restrictions. These results show that addition of epigenetic agents, such as cladribine and HDACis, to alemtuzumab treatment overcomes resistance to alemtuzumab in T-PLL. Resistance and subsequent re-sensitization to alemtuzumab was not caused by the silencing and then re-expression of CD52 after treatment (fig. S4). Major toxicities were hematologic and immune suppression. One patient experienced a fatal CNS hemorrhage, a potential rare complication of

T-PLL and alemtuzumab therapy (33) (table S2). Of the eight patients, five died with persistent disease, one remains in remission after allogeneic transplant, and two remain alive in early relapse (Table 1).

Induction of CD30 gene expression and changes in CD30 promoter chromatin marks after epigenetic therapy in T-PLL patients

The addition of cladribine induced the expression of CD30 in three patients after initial treatment (Fig. 3). One more patient expressed CD30 after switching from vorinostat to romidepsin after first relapse (figs. S3 and S4). Two patients (1 and 5) were then successfully treated with brentuximab vedotin. We did not observe increases in CD30 in four MCL patients after treatment with epigenetic drugs, indicating that CD30 induction is specific to T-PLL (fig. S5).

To further explore the transcriptional effect of epigenetic drugs on *TNFRSF8* (CD30), we carried out chromatin immunoprecipitation (ChIP) assays. We analyzed the –100- to –1-bp regions upstream of the transcription start site from patients 1 and 5. These two patients were chosen, because they showed CD30 induction and were successfully treated with brentuximab

Fig. 3. Epigenetic therapy induced *CD30* gene expression and chromatin reorganization. (A) Patient mRNA samples were assayed for *CD30* gene expression using quantitative reverse transcription PCR (qRT-PCR) before and 5 days after treatment with epigenetic therapy. Fold change represents the fold increase or decrease of expression after treatment relative to before treatment. Numbers in parentheses indicate actual fold change. (B and C) Genomic DNA from patients 1 (B) and 5 (C) was assessed for changes in DNA and chromatin methylation as well as RNA Pol II binding before and after treatment using CHIP assays. For patient 5, samples were taken before and 5 days after treatment of relapse with romidepsin instead of vorinostat. For patient 1, samples were taken before and 5 days after initial epigenetic treatment. Fold change indicates fold increase or decrease in binding after treatment as measured by qRT-PCR. Three regions of the *CD30* promoter were considered in this assay spanning roughly 400 bp on each side of the transcription start site. Prox refers to a 200-bp region around the transcription start site. * $P < 0.05$, ** $P < 0.005$, *** $P < 0.0005$. Bars represent mean fold change \pm SEM. $n = 3$.

vedotin. There were increases in RNA polymerase II (Pol II) binding as well as decreased amounts of methylated cytosine residues [5-methylcytosine (5mC)], histone 3 lysine 9 trimethylation (H3K9Me3), and histone 3 lysine 27 trimethylation (H3K27Me3) after treatment (Fig. 3, B and C).

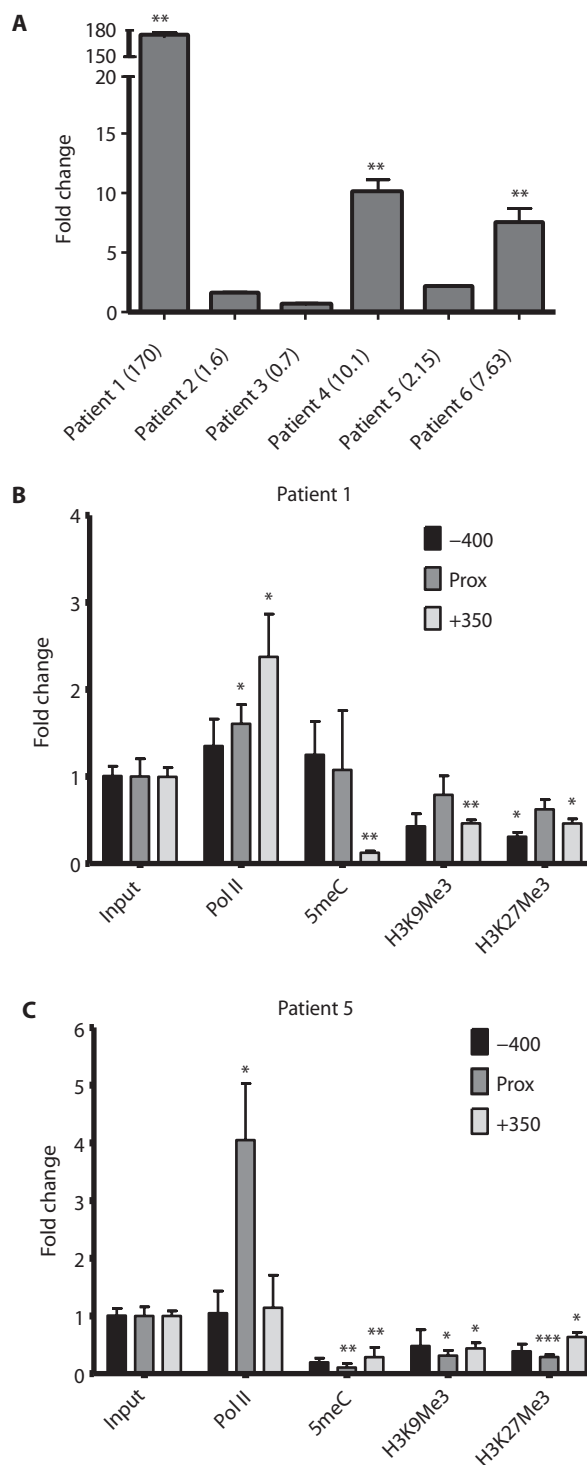
Alemtuzumab-resistant skin lesions treated with brentuximab vedotin and epigenetic drugs

Patient 5 relapsed with both leukemic and dermatologic infiltration by prolymphocytes. He initially underwent treatment with alemtuzumab, cladribine, and vorinostat. After 2 months of treatment, he achieved CR (fig. S3). After 6.3 months of remission, he relapsed and did not respond to treatment. At this time, vorinostat was replaced with romidepsin, and the patient achieved a second remission lasting 4 months.

At the time of his second relapse, he showed a resurgence of leukemic cells as well as infiltration of prolymphocytes into the dermis of the skin. He was treated again with alemtuzumab, cladribine, and romidepsin. His peripheral blood counts responded, but his skin did not. Lymphocytes in both compartments remained CD52-positive (fig. S6). The patient's skin disease was progressing and was refractory to treatment with alemtuzumab, vorinostat, and romidepsin. Pralatrexate was tried, because it is approved for use in T cell malignancies. It also had no effect. A biopsy showed dermis-infiltrating lymphocytes testing weakly positive for CD30 surface expression (Fig. 5A). His peripheral disease tested positive for CD30 throughout his second relapse as well (Fig. 4). He was subsequently started on brentuximab vedotin. His skin scabbed and cleared over the next month. Repeat biopsy of a healing skin lesion showed lymphocyte depletion (Fig. 5B). He remained in remission for 5 months. Shortly thereafter, his lymphocyte count began to increase again, from 1180 to 5500 (Fig. 4). They were found to be CD30⁺, CD52⁺ (Fig. 4, inset). Alemtuzumab was initiated again. In the interim, the patient was human leukocyte antigen (HLA)-typed and received an allogeneic stem cell transplant complicated by graft-versus-host disease with persistent lymphadenopathy and died shortly thereafter.

mRNA microarray and qRT-PCR analyses of lymphocyte proliferation after epigenetic treatment

Microarray analysis before and after epigenetic therapy was performed on four patients from whom there was a sufficient amount of quality



RNA (fig. S7). Genes were filtered, using a twofold increase in expression after treatment as the cutoff. Targets that showed increases in two or more patients after therapy were confirmed by qRT-PCR. The genes with the most highly increased expression after epigenetic therapy were interferon-inducible proteins and mediators of mitogen-activated protein kinase (MAPK) activity, mainly the HIN-200 and

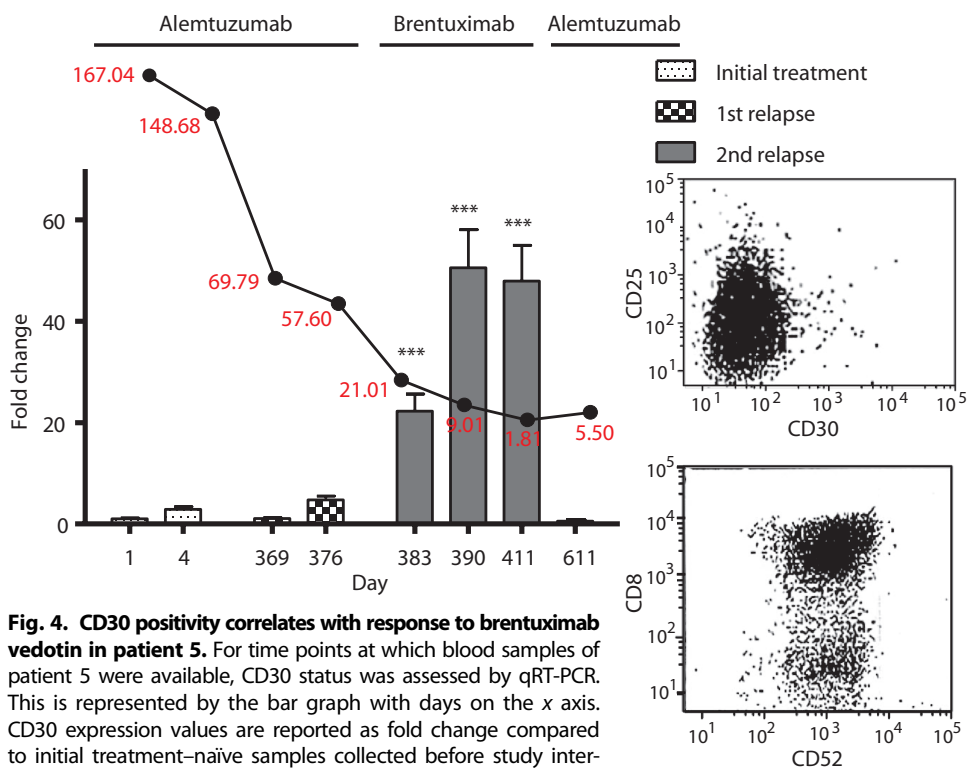


Fig. 4. CD30 positivity correlates with response to brentuximab vedotin in patient 5.

For time points at which blood samples of patient 5 were available, CD30 status was assessed by qRT-PCR. This is represented by the bar graph with days on the x axis. CD30 expression values are reported as fold change compared to initial treatment-naïve samples collected before study intervention. White blood cell counts (in red) from these same time points were also collected and graphed above their corresponding dates (black line graph). Antibody treatment received during each period is labeled above the graph. Switch from vorinostat to romidepsin occurred around day 200. The inset to the right shows flow cytometry data of CD30-negative (top) and CD52-positive (bottom) cell populations at the last time point at which CD30 expression was observed to disappear by qRT-PCR, after which treatment was switched back to alemtuzumab. *** $P < 0.0005$. Bars represent mean fold change \pm SEM. $n = 3$.

CCAAT ester-binding protein (CEBP) families. We studied the HIN-200 family because of its known relevance to tumor biology and sequential location on chromosome 1q21-23 (34). All four members of the HIN-200 family—*MNDA*, *IFI16*, *PYHIN*, and *AIM2*—were assayed for expression changes by qRT-PCR after treatment. Not all patient samples up-regulated the same family member, but they all up-regulated at least one of the four (Fig. 6). The CEBP family contains six members: *CEBPA*, *CEBPB*, *CEBPD*, *CEBPE*, *CEBPG*, and *CEBPZ*. *CEBPA*, *CEBPB*, and *CEBPD* have distinct functions (35). As with the HIN-200 family, not all posttreatment samples up-regulated the same CEBP gene, but they all up-regulated at least one family member after treatment (Fig. 6). After microarray analysis of patients' mRNA expression after therapy, *TRIB1*, which codes for the tribbles-1 protein, was the only gene that showed at least twofold increase in expression in all four tested patients. qRT-PCR confirmed that four of six T-PLL patients up-regulated *TRIB1* expression (Fig. 7A). ChIP assays on the *TRIB1* promoter of samples from patients 1 and 5 showed increases in RNA Pol II and pan-H4 acetylation, and corresponding decreases in H3K9Me3. Patient 5 showed more pronounced increases in Pol II and pan-H4 acetylation than did patient 1 and large decreases in 5meC, H3K9Me3, and H3K27Me3 (Fig. 7B). These changes are consistent with decreased repressive chromatin marks (36). Microarray data also suggested that globin genes, *HBA* and *HBB*, were up-regulated (fig. S7). qRT-PCR of these genes confirmed the microarray results. All patient samples except for pa-

tients 3 and 4 showed increases in globin mRNA expression after treatment (Fig. 6).

We also used qRT-PCR to assess other candidate genes involved in the biology of T-PLL after treatment. *BAX*, *ATM*, *CDKN1B* (p27), *TCL1*, *MTCPI1*, and *DUSP16* are known to have aberrant expression in T-PLL in general (37–41). We found mRNA expression of *TCL1* and *CDKN1B* to be abnormal in our patients. Patients 1, 2, 3, and 5 showed overexpression of *TCL1* (fig. S8), which is overexpressed in 70% of T-PLL (2). All patients showed less than half the amount of *CDKN1B* mRNA relative to normal controls, in line with published reports that p27 haploinsufficiency plays a critical role in T-PLL pathogenesis (fig. S8) (37). Aberrations in expression of these genes did not change after treatment with epigenetic drugs, indicating that though important, these elements of T-PLL tumor biology are not epigenetically regulated in our patients. However, the presence of these dysregulated genes confirms the T-PLL signature in the microarray data.

STAT5B mutational status of T-PLL patients

All patients were tested for the N642H *STAT5B* (signal transducer and activator of transcription 5B) mutation by PCR amplification and DNA sequencing. Additionally, DNA banked from two previ-

ous T-PLL patients (402 and 429) not on our study was sequenced for this mutation as well. Six of 10 (60%) were wild-type *STAT5B*, 3 of 10 (30%) were heterozygous for the N642H mutation, and 1 of 10 (10%) was homozygous for the mutation (fig. S9).

DISCUSSION

We found that eight patients with T-PLL responded to combination therapy with alemtuzumab and epigenetic agents. The median survival after first relapse, censored for living patients (patients 6 to 8), was 13 months, and the median overall survival was 15.3 months. Toxicities experienced by the patients were mainly infectious in nature and managed with conventional monitoring and antibiotic therapy. One patient did experience a fatal CNS hemorrhage, which may have been related to therapy. Although the patient numbers are small, it is interesting to look at overall survival in our patients stratified by previous therapy. Two patients initially resistant to alemtuzumab had overall survival of 34.3 and 12+ months (patients 1 and 7, respectively), compared to an expected survival of 4 months in such patients (5, 42). Patient 2, who had relapsed after initial alemtuzumab therapy, had an overall survival of 17 months, compared to expected survival of between 7.5 and 10 months. Patient 8 was also treated after initial alemtuzumab relapse and has survived 23.7+ months (5, 9, 43). Four of our

Fig. 5. Brentuximab vedotin cleared CD30⁺ skin lesions in patient 5. (A) Immunohistochemistry (IHC) of biopsies of these lesions showed CD30⁺ infiltrate (left) in the dermis before treatment with brentuximab vedotin and absent CD30⁺ T-PLL cells after 2 months of treatment (right). Blue, nucleus; brown, CD30. Scale bars, 20 μ m. (B) Images of the upper left shoulder (top) and lateral left chest wall (bottom) depict plaques infiltrated with CD30⁺ T-PLL cells before (left) and after (right) treatment with brentuximab vedotin.

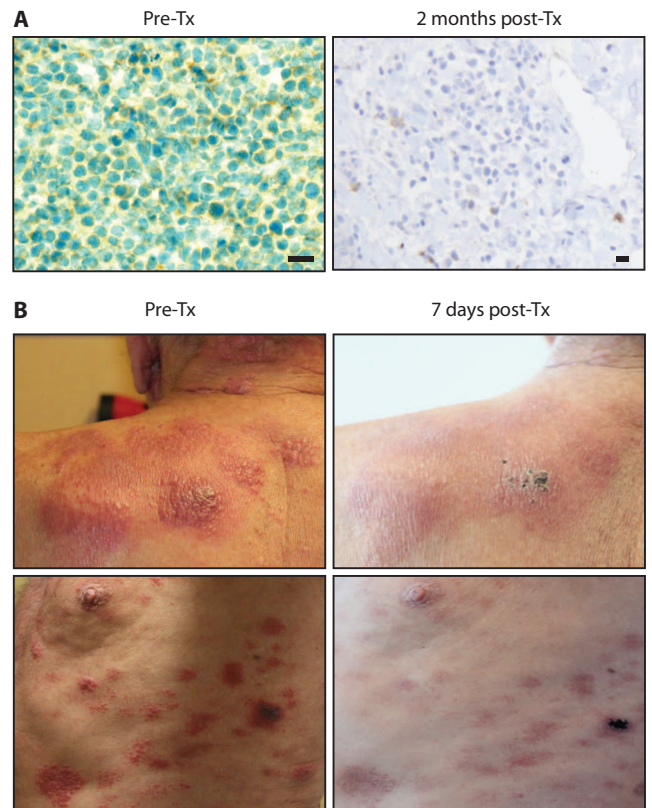
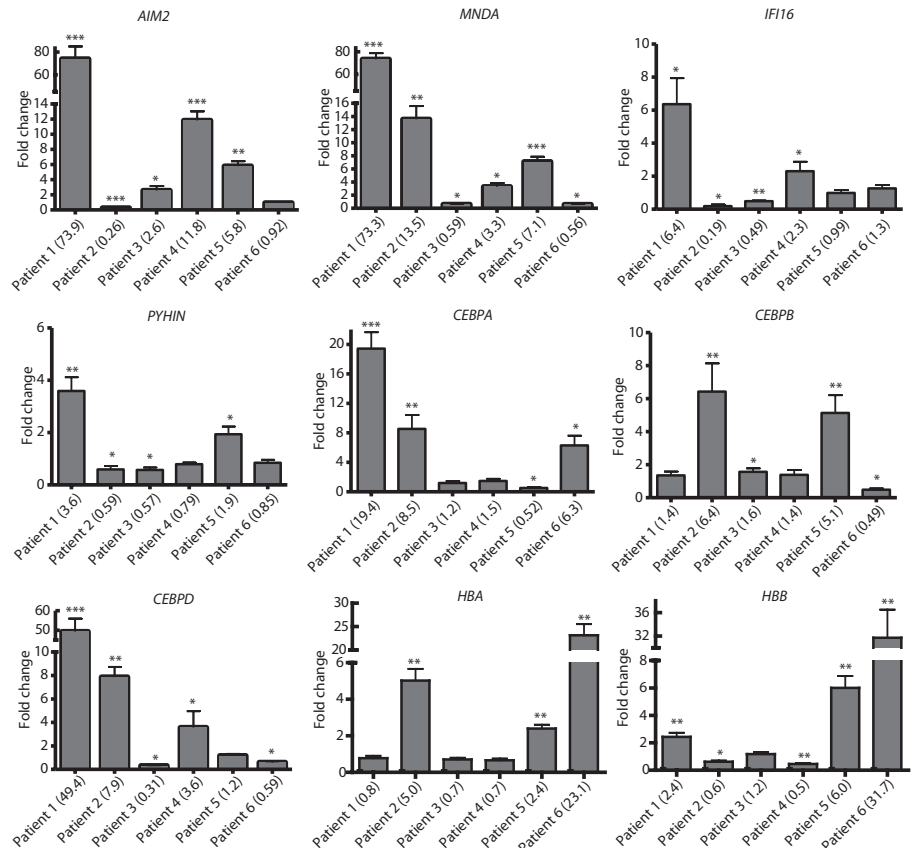


Fig. 6. Epigenetic therapy induces HIN-200, CEBP, and globin gene expression. Changes in expression of *AIM2*, *MNDA*, *IFI16*, *PYHIN*, *CEBPA*, *CEBPB*, *CEBPD*, *HBA*, and *HBB* were assessed by qRT-PCR before and 5 days after treatment of six patients with epigenetic therapy. Sufficient samples for mRNA analysis were only available for patients 1 to 6. Only three CEBP family members were tested. Values are shown as fold changes as compared to treatment-naïve expression in each patient. Numbers in parentheses indicate actual fold change. * $P < 0.05$, ** $P < 0.005$, *** $P < 0.0005$. Bars represent mean fold change \pm SEM. $n = 3$.



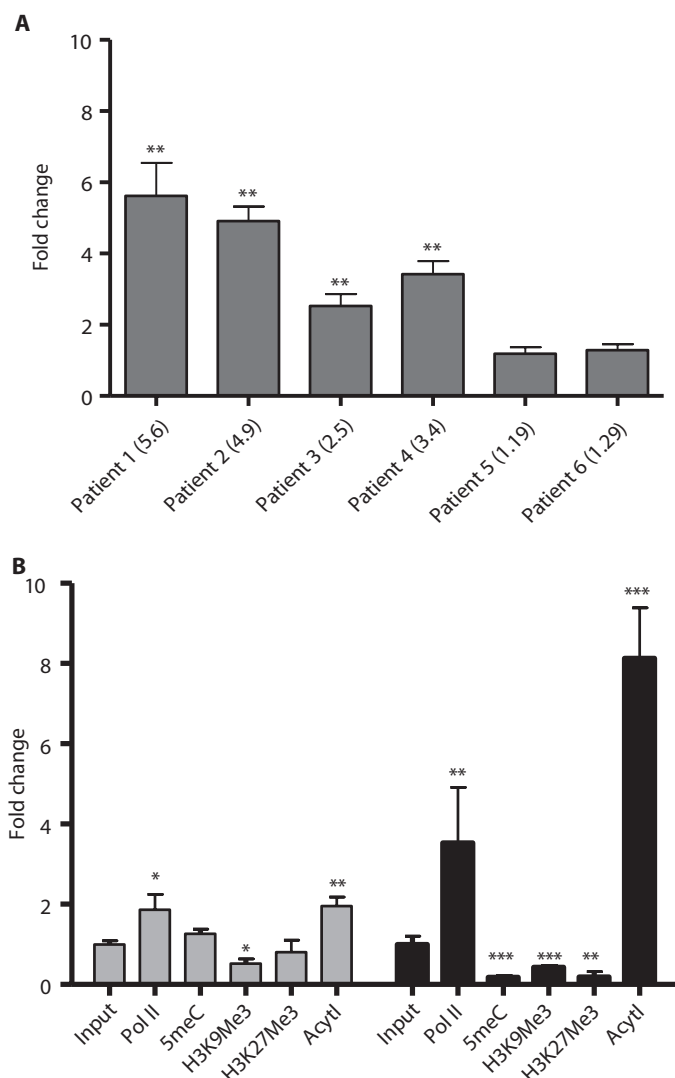


Fig. 7. Epigenetic therapy induces *TRIB1* expression and increases active chromatin marks. (A) Changes in expression of *TRIB1* were assessed by qRT-PCR before and after treatment of six patients with epigenetic therapy. Values are shown as fold changes as compared to treatment-naïve expression in each patient. Numbers in parentheses indicate actual fold change. (B) Genomic DNA from patients 1 (gray) and 5 (black) was assessed with ChIP to detect changes in DNA and chromatin methylation as well as RNA Pol II binding before and 5 days after treatment, the same time points as in Fig. 3 (B and C). Fold change indicates fold increase or decrease in binding after treatment as measured by qRT-PCR. The region represented is 400 bp around the transcriptional start of the *TRIB1* gene. Acetyl, pan-histone acetylation. * $P < 0.05$, ** $P < 0.005$, *** $P < 0.0005$. Bars represent mean fold change \pm SEM. $n = 3$.

patients were treated initially with a combination epigenetic therapeutic approach. One remains in remission after allogeneic transplant. Survival times of the other patients were 5.7, 14.8, and 15.3 months compared to overall survival of 20 months for patients treated with initial alemtuzumab alone (5). These data suggest that addition of epigenetic therapy might be best suited for patients with alemtuzumab-refractory or relapsed disease.

Treatment with these drugs showed an altered mRNA expression profile on microarray analysis, implicating the CEBPs, HIN-200 family, and tribbles (*TRIB1*) proteins in epigenetic dysregulation during malignancy. The epigenetic treatment regimen activated expression of CD30 in four patients; two then received successful treatment with brentuximab vedotin. These findings represent a potential effective treatment paradigm for T-PLL.

We hypothesize that cladribine and HDACis may activate effector cells such as natural killer (NK) and T cells or granulocytes to enhance the antitumor effects of alemtuzumab through ADCC and reexpress silenced genes. The absence of apoptotic changes in T-PLL cells after treatment supports enhanced ADCC. The increases in CD30 expression and decreases in CD30 promoter histone and DNA methylation observed after treatment point to epigenetic silencing in T-PLL. Despite these findings, the full mechanism by which epigenetic agents induce the expression of CD30 has not been fully elucidated. The two patients in whom CD30 induction was not observed were treated with alemtuzumab, cladribine, and vorinostat. The presence of vorinostat most likely silenced the expression of CD30. This observation is consistent with in vitro findings from our laboratory that vorinostat can transiently ablate CD30 expression (44). This is further supported by the additional observation that patient 5 showed no CD30 up-regulation until he was switched from vorinostat to romidepsin. These data support the ability of combined epigenetic and immunotherapy to modulate gene expression in T-PLL.

Induction of CD30 provides an additional method to circumvent resistance in T-PLL. Patients 1 and 5 were successfully treated with brentuximab vedotin after epigenetic induction of CD30. Treatment with brentuximab vedotin was only considered in patients who showed CD30 up-regulation and had exhausted epigenetic treatment options because of treatment failure or toxicity (patients 1 and 5). Their response to treatment indicates that epigenetic therapy not only overcame resistance to alemtuzumab but also generated sensitivity to another drug class. This finding proved important for treatment of patient 5's skin lesions, because his blood responded to treatment with alemtuzumab but his skin did not. Certain aspects of the dermal environment were likely not conducive to alemtuzumab function despite CD52 positivity. Clark *et al.* showed that leukemia cells that do not reenter blood circulation in CTCL are resistant to alemtuzumab despite CD52 positivity and alemtuzumab penetration into the dermis (45). Regardless of the mechanism, epigenetic therapy enabled the use of brentuximab vedotin to circumvent alemtuzumab resistance in skin lesions in this T-PLL patient.

Correlative experiments found three up-regulated gene families that potentially link dysregulation of the MAPK and interferon pathways with the extreme proliferative drive of T-PLL. These two pathways can be connected by CEBP family transcription factors, particularly CEBPB. CEBPB is induced by interferon γ and is required to activate expression of death-associated protein kinase 1 (DAPK1), a protein that regulates the cell cycle and apoptosis (46). DAPK1 induction by CEBPB requires extracellular signal-regulated kinase (ERK) signaling (46, 47). The tribbles family of proteins, mainly *TRIB1*, regulates MAPK signaling through scaffold-like interactions of MAPK kinase (MEK) and ERK, and interacts with CEBPB (48–50). Increased expression of these two gene families after epigenetic therapy could help to reinitiate apoptosis and slow cell growth. The HIN-200 family of genes also links growth-suppressing interferon pathways to T-PLL by acting as regulators of cell cycle progression and differentiation and therefore tumor suppressor proteins (51, 52). Reversal of HIN-200 silencing through epigenetic therapy could resensitize cells to death signals. Overall, reexpression of the

HIN-200, CEBP, and tribbles families may contribute to the dramatic fall in circulating leukemia cells after epigenetic treatment through re-gaining control of the cell cycle.

The N642H *STAT5B* mutation has been identified in several types of aggressive T cell lymphomas, including T cell large granular lymphocyte leukemia (T-LGL) where it was discovered (53), pediatric acute lymphoblastic leukemia (54), and aggressive NK cell lymphomas (55). Because T-PLL presents as an aggressive disease (high white blood cell counts, organomegaly, cytopenias, skin manifestations, etc.), we hypothesized that *STAT5B* mutations may be present in T-PLL as well. The T to G point mutation replaces an asparagine with a histidine at position 642 in the Src-like homology 2 domain. This change leads to hyperactivated *STAT5B* (53). We noted that 4 of 10 (40%) of our patients carried the mutation in their leukemic clone. The presence of the mutation did not seem to have an effect on the efficacy of epigenetic therapy. A recent study from Kiel *et al.* showed that *STAT5B* was hyperactive in T-PLL in general and that targeted inhibition of *STAT5B* promoted apoptosis (56). Similarly to the gene families found up-regulated after epigenetic therapy, hyperactivated *STAT5B* with the N642H mutation dysregulates interferon signaling and the Janus kinase/STAT pathway. This mutation further implicates the interferon pathway in the aggressiveness of T-PLL. Our findings suggest that targeting the interferon pathway, potentially through development of anti-N642H *STAT5B* therapeutics, may have merit in the treatment of T-PLL.

Our study has several limitations, particularly regarding the relatively small sample size. We were only able to obtain blood samples before and after epigenetic treatment from six of the eight patients. All patients received some form of epigenetic therapy, but the epigenetic drugs varied somewhat. Although correlative studies identified gene families that were up-regulated with epigenetic therapy, we were unable to definitively determine the mechanism that governed the susceptibility of T-PLL to such therapy. The promising results of this pilot study need validation in a larger prospective trial.

This study presents an effective epigenetic combination drug therapy for T-PLL, an aggressive T cell leukemia for which there are few treatment options and a poor prognosis. Such therapy appears to overcome drug resistance. Although patients eventually relapsed, leukemia cells at relapse remained sensitive to this regimen. The reinduction of complete remission in resistant disease creates multiple opportunities to pursue curative therapy with allogeneic stem cell transplant. The most clinically relevant epigenetic change noted was the induction of drug target CD30. This observation formed the basis for successful treatment with brentuximab vedotin. We suggest that the combination of cladribine with or without an HDACi and an appropriate tumor-specific monoclonal antibody may be an important therapeutic platform for the treatment of cancer.

MATERIALS AND METHODS

Study design

This was a pilot study performed under the supervision of the two senior authors primarily at one institution. Because of the rarity of T-PLL, eight patients were studied over the course of 7 years. Diagnosis of T-PLL was made on the basis of immunophenotype, peripheral blood smear, clinical presentation, and laboratory values as outlined previously (5). Complete remission was defined as the absence of disease detectable by morphology and resolution of splenomegaly/

lymphadenopathy confirmed by physical examination and/or computed tomography (CT) scanning. Repeat bone marrow samples were not obtained in all patients. Molecular remission was defined as both negative flow cytometry for minimal residual disease and no detectable clone by T cell receptor rearrangement analysis using PCR. Partial remissions were defined as 50% or more decrease in circulating tumor cell counts but lack of normalization of other complete remission criteria (5, 9, 42, 43). Patients with lymphadenopathy or splenomegaly were followed by CT scans (table S1). Patients were treated until they achieved remission (one to three cycles), opted to end therapy, or received an allogeneic bone marrow transplant. The end point of this study was allogeneic transplant or death. The objective of this study was to determine whether epigenetic therapies could overcome treatment resistance in T-PLL. One cycle of therapy was 28 days and defined as follows (Fig. 1): alemtuzumab given at 30 mg intravenously on days 1, 3, 5, 8, 10, 12, 15, 17, 19, 22, 24, and 26; cladribine given at 5 mg/m² on days 1 to 5; and vorinostat given orally at 400 mg a day on days 1 to 5. Romidepsin was dosed at 14 mg/m² on days 1, 8, and 15 when used. In the case of CD30 induction and treatment with brentuximab vedotin, 1.8 mg/kg once a week for 3 weeks was used. Pralatrexate dose was 30 mg/m² intravenously. Patients 1, 3, 4, and 6 were treated with two to three cycles of therapy with only alemtuzumab and cladribine. If white blood cell counts did not respond, vorinostat was added. After noting that the addition of vorinostat led to better responses, vorinostat was routinely added with alemtuzumab and cladribine, given that hematologic and infectious toxicities were manageable with supportive care. Alemtuzumab was continued three times a week for 2 weeks after patients achieved CR. No maintenance alemtuzumab was used because of the risk of opportunistic infections and lack of added benefit (5). Patients were prophylaxed for infectious complications with sulfamethoxazole/trimethoprim, levofloxacin if neutropenic, and daily acyclovir, and monitored for infections, especially cytomegalovirus. Clinical data collected were white blood cell counts, molecular and flow cytometric analyses of the blood and bone marrow, skin biopsies, and toxicities. Six of the eight patients were consented for collection of blood under a Penn State Hershey Institutional Review Board-approved protocol (no. 2000-186). Blood was collected before initiating therapy, at days 3 and 5 after therapy. The remaining two patients were treated at other institutions and were not consented for blood collection during their initial treatments. Blood samples from the six consented patients were used for correlative laboratory studies.

White blood cell separation

White blood cells were separated from blood on Ficoll-Paque PLUS (GE Healthcare) gradients and lysed to extract protein, DNA, or RNA. Remaining cells were stored in highly concentrated aliquots (>10⁷ cells) in fetal bovine serum (FBS) with 10% dimethyl sulfoxide (DMSO) in locked liquid N₂ dewars (-195°C).

Patient photographs

After obtaining written consent, patient photographs were taken using a Canon T2i camera.

Flow analyses and IHC

All clinical flow analyses and IHC analyses of skin biopsies were carried out by the Penn State Hershey Department of Pathology. IHC was done on a Ventana Benchmark XT automated immunoperoxidase stainer. Briefly, slides were cut from paraffin-embedded tissue

blocks and deparaffinized. Cells were conditioned in buffer (pH 8.0) for 30 min before addition of CD30 antibody at 1:100 dilution for 24 min. Slides were then blocked in avidin/biotin blocker and counter stained with hematoxylin and eosin stain.

mRNA microarray analysis

mRNA microarray analysis was carried out using a microarray chip (Illumina) and the facilities of the Penn State Genomics Core. Complementary DNA (cDNA) was made from mRNA extracted from four patients before and after therapy using High-Capacity cDNA Reverse Transcription Kits (Applied Biosystems). Only four of the six patients had sufficient quality mRNA for microarray experimentation. Results were analyzed using MS Excel and gene set enrichment analysis from the Broad institute.

Quantitative RT-PCR

White blood cells were isolated, washed, and lysed in TRIzol (Ambion) as per the manufacturer's instructions. All RNA was then subjected to RQ1 ribonuclease-free deoxyribonuclease (DNase) (Promega) to eliminate residual DNA. After DNase treatment, samples were reverse-transcribed, and qRT-PCR was carried out using SYBR Green (Qiagen) and BLAST designed primers (IDT). Primer sequences can be found in table S3.

ChIP assays

Frozen (90% FBS and 10% DMSO) patient cells were thawed and suspended in 10 ml of phosphate-buffered saline (PBS) and fixed in 0.4% formaldehyde for 10-min rocking at room temperature. Fixation was stopped by 500 μ l of 2.5 M glycine for 5 min, followed by cold PBS wash. Cells were suspended in 500 μ l of cold lysis buffer (50 mM tris, 10 mM EDTA, and 1% SDS) with 1:100 protease inhibitor cocktail (Sigma P8340) and incubated on ice for 30 min. Lysates were sonicated using a Misonix Microson XL at 25% power for six cycles of 30 s on, 30 s off, and incubated on ice. Insoluble material was cleared with a 10-min, 17,000g spin. Fifty microliters of input chromatin was diluted to 500 μ l in dilution buffer (20 mM tris, 2 mM EDTA, 150 mM NaCl, and 1% Triton X-100). Fifteen microliters of Magna ChIP Protein A+G beads (Millipore) was added, as well as 10 μ g of antibody against the desired target. Antibodies used were as follows: H3 lysine 27 trimethyl (Millipore 05-1951), H3 lysine 9 trimethyl (Millipore 07-523), normal rabbit antibody (Santa Cruz Biotechnology sc-2345), or histone H3 positive control antibody (Cell Signaling #9715). Mixtures were precipitated overnight at 4°C with rotation, then washed with 750 μ l of the following buffers, each with 5-min incubation at 4°C with rotation: low-salt buffer (50 mM NaCl, 0.1% SDS, 1% Triton X-100, 10 mM tris-HCl, 1 mM EDTA), high-salt buffer (150 mM NaCl, 0.1% SDS, 1% Triton X-100, 10 mM tris-HCl, 1 mM EDTA), LiCl buffer (250 mM LiCl, 1% deoxycholic acid, 1% NP-40, 10 mM tris-HCl, 1 mM EDTA), and twice with TE (10 mM tris-HCl, 1 mM EDTA). After washes, chromatin was eluted from beads in 100 μ l of elution buffer (1% SDS, 100 mM NaHCO₃) plus 1 μ l of proteinase K (Qiagen) at 64°C overnight. Eluted DNA was purified using a PCR Purification Kit (Qiagen). DNA was detected by qRT-PCR with a QuantiTect SYBR Green PCR Kit (Qiagen) on a Bio-Rad C1000 real-time thermocycler. All ChIP assay PCRs were done in triplicate and independently repeated at least twice.

STAT5B N642H sequencing

Sequencing for the N642H *STAT5B* mutation was carried out using genomic DNA from patients as a template. *STAT5B* mutation forward

and reverse primers (table S3), spanning an ~250-bp region, were used to amplify out the mutation site using Takara Hot Start Taq polymerase (Clontech). The reaction was PCR-purified (Qiagen) and sent for sequencing (Fisher/Operon) using the *STAT5B* mutation reverse primer. Paired normal germline controls were unavailable.

DNA methylation analysis by HELP

Genomic DNA was isolated using a standard high-salt procedure. HELP assay, a comparative isoschizomer profiling method interrogating cytosine methylation status on a genomic scale, was carried out as previously described (57–59). Briefly, genomic DNA from the samples was digested by a methylcytosine-sensitive enzyme, Hpa II, and by a methylcytosine-insensitive enzyme, Msp I. The Hpa II- and Msp I-digested products were amplified by ligation-mediated PCR optimized to amplify fragments between 200 and 2000 bp with the preferential amplification of cytosine-phosphate-guanosine (CpG) dinucleotide-dense regions. Each fraction was then labeled with a specific dye and cohybridized onto a human HG17 custom-designed oligonucleotide array (50-mers) covering 25,626 Hpa II amplifiable fragments (HAFs) located at gene promoters and imprinted regions across the genome (58). HAFs are defined as genomic sequences between two flanking Hpa II sites found within 200 to 2000 bp from each other. Each HAF on the array is represented by 15 individual probes. All samples for microarray hybridization were processed at the Roche-NimbleGen Service Laboratory. PCR fragment length bias was corrected by quantile normalization. Further quality control and data analysis of HELP microarrays were performed as described by Thompson *et al.* (60).

TUNEL assay

T-PLL cells were attached to glass slides using a cytospin at 500 rpm for 5 min before processing and staining with the Click-iT TUNEL Alexa Fluor Imaging assay (Invitrogen C10245) and accompanying protocol, then imaged on an Olympus BX60 upright fluorescence microscope.

Statistical analyses

All significant *P* values were derived from two-tailed Student's *t* tests with a cutoff of *P* < 0.05 and can be found in table S4. All experiments were repeated twice. Survival times were calculated from the start of therapy.

SUPPLEMENTARY MATERIALS

www.sciencetranslationalmedicine.org/cgi/content/full/7/293/293ra102/DC1

Supplemental patient case information

Fig. S1. Cladribine inhibits DNA methylation in vivo and histone methylation in vitro.

Fig. S2. Epigenetic therapy does not induce apoptosis in T-PLL.

Fig. S3. Epigenetic therapy lowered leukemic white blood cell counts despite multiple relapses.

Fig. S4. *CD52* expression was unchanged by epigenetic therapy.

Fig. S5. *CD30* induction was not observed in circulating MCL cells.

Fig. S6. Skin biopsy from patient 5 shows *CD52*-positive dermis-infiltrating lymphocytes.

Fig. S7. Epigenetic treatment of T-PLL causes mRNA expression changes in the HIN-200, CEBP, and tribbles families.

Fig. S8. All tested patients showed *CDKN1B* haploinsufficiency, and four of six were *TCL1*-positive.

Fig. S9. Forty percent of patients were positive for the N642H *STAT5B* mutation.

Table S1. Patient presentation at diagnosis.

Table S2. Patient characteristics and adverse events.

Table S3. Primer sequences.

Table S4. Significant *P* values for all statistically significant comparisons in figures.

References (61, 62)

REFERENCES AND NOTES

1. T. Robak, P. Robak, Current treatment options in prolymphocytic leukemia. *Med. Sci. Monit.* **13**, RA69–RA80 (2007).
2. C. E. Dearden, T-cell prolymphocytic leukemia. *Med. Oncol.* **23**, 17–22 (2006).
3. E. Matutes, V. Brito-Babapulle, J. Swansbury, J. Ellis, R. Morilla, C. Dearden, A. Sempere, D. Catovsky, Clinical and laboratory features of 78 cases of T-prolymphocytic leukemia. *Blood* **78**, 3269–3274 (1991).
4. R. Pawson, T. F. Schulz, E. Matutes, D. Catovsky, The human T-cell lymphotropic viruses types I/II are not involved in T prolymphocytic leukemia and large granular lymphocytic leukemia. *Leukemia* **11**, 1305–1311 (1997).
5. C. Dearden, How I treat prolymphocytic leukemia. *Blood* **120**, 538–551 (2012).
6. J. Mercieca, E. Matutes, C. Dearden, K. MacLennan, D. Catovsky, The role of pentostatin in the treatment of T-cell malignancies: Analysis of response rate in 145 patients according to disease subtype. *J. Clin. Oncol.* **12**, 2588–2593 (1994).
7. S. Spurgeon, M. Yu, J. D. Phillips, E. M. Epner, Cladribine: Not just another purine analogue? *Expert Opin. Investig. Drugs* **18**, 1169–1181 (2009).
8. L. Ginaldi, M. De Martinis, E. Matutes, N. Farahat, R. Morilla, M. J. Dyer, D. Catovsky, Levels of expression of CD52 in normal and leukemic B and T cells: Correlation with in vivo therapeutic responses to Campath-1H. *Leuk. Res.* **22**, 185–191 (1998).
9. M. J. Keating, B. Cazin, S. Coutre, R. Birhayer, T. Kovacsovic, W. Langer, B. Leber, T. Maughan, K. Rai, G. Tjønnfjord, M. Bekradda, M. Itzhaki, P. Hérait, Campath-1H treatment of T-cell prolymphocytic leukemia in patients for whom at least one prior chemotherapy regimen has failed. *J. Clin. Oncol.* **20**, 205–213 (2002).
10. H. Y. Lin, C. S. Chen, S. P. Lin, J. R. Weng, C. S. Chen, Targeting histone deacetylase in cancer therapy. *Med. Res. Rev.* **26**, 397–413 (2006).
11. H. Fukuda, N. Sano, S. Muto, M. Horikoshi, Simple histone acetylation plays a complex role in the regulation of gene expression. *Brief. Funct. Genomic. Proteomic.* **5**, 190–208 (2006).
12. D. Wyczechowska, K. Fabianowska-Majewska, The effects of cladribine and fludarabine on DNA methylation in K562 cells. *Biochem. Pharmacol.* **65**, 219–225 (2003).
13. H. Gowher, A. Jeltsch, Mechanism of inhibition of DNA methyltransferases by cytidine analogs in cancer therapy. *Cancer Biol. Ther.* **3**, 1062–1068 (2004).
14. O. Khan, N. B. La Thangue, HDAC inhibitors in cancer biology: Emerging mechanisms and clinical applications. *Immunol. Cell Biol.* **90**, 85–94 (2012).
15. E. E. Cameron, K. E. Bachman, S. Myröhänen, J. G. Herman, S. B. Baylin, Synergy of demethylation and histone deacetylase inhibition in the re-expression of genes silenced in cancer. *Nat. Genet.* **21**, 103–107 (1999).
16. S. Y. Lee, C. G. Park, Y. Choi, T cell receptor-dependent cell death of T cell hybridomas mediated by the CD30 cytoplasmic domain in association with tumor necrosis factor receptor-associated factors. *J. Exp. Med.* **183**, 669–674 (1996).
17. S. Han, J. Koo, J. Bae, S. Kim, S. Baik, M. Y. Kim, Modulation of TNFSF expression in lymphoid tissue inducer cells by dendritic cells activated with Toll-like receptor ligands. *BMB Rep.* **44**, 129–134 (2011).
18. P. Biswas, A. Galli, B. Capiluppi, D. Ciuffreda, A. Lazzarin, G. Tambussi, Selective enrichment of CD30-expressing cells within the blast region of lymphocytes from patients with primary HIV infection (PHI). *J. Biol. Regul. Homeost. Agents* **16**, 33–36 (2002).
19. D. Saini, S. Ramachandran, A. Nataraju, N. Benshoff, W. Liu, N. Desai, W. Chapman, T. Mohanakumar, Activated effector and memory T cells contribute to circulating sCD30: Potential marker for islet allograft rejection. *Am. J. Transplant.* **8**, 1798–1808 (2008).
20. M. A. Halim, T. Al-Otaibi, I. Al-Muzairi, M. Mansour, K. A. Tawab, W. H. Awadain, M. A. Balaha, T. Said, P. Nair, M. R. Nampoory, Serial soluble CD30 measurements as a predictor of kidney graft outcome. *Transplant. Proc.* **42**, 801–803 (2010).
21. E. Kocabaş, A. Türel Emertcan, S. Akinci, P. Temiz, K. Gündüz, Primary cutaneous CD30-positive anaplastic large cell lymphoma in a 16-year-old girl. *Int. J. Dermatol.* **51**, 1353–1358 (2012).
22. R. Hussain, A. Bajoghli, Primary cutaneous CD30-positive large T-cell lymphoma in an 80-year-old man: A case report. *ISRN Dermatol.* **2011**, 634042 (2011).
23. I. Maric, K. R. Calvo, Mastocytosis: The new differential diagnosis of CD30-positive neoplasms. *Leuk. Lymphoma* **52**, 732–733 (2011).
24. M. Tarkowski, Expression and a role of CD30 in regulation of T-cell activity. *Curr. Opin. Hematol.* **10**, 267–271 (2003).
25. J. A. Francisco, C. G. Cervený, D. L. Meyer, B. J. Mixan, K. Klussman, D. F. Chace, S. X. Rejniak, K. A. Gordon, R. DeBlanc, B. E. Toki, C. L. Law, S. O. Doronina, C. B. Siegall, P. D. Senter, A. F. Wahl, cAC10-vcMMAE, an anti-CD30-monomethyl auristatin E conjugate with potent and selective antitumor activity. *Blood* **102**, 1458–1465 (2003).
26. S. O. Doronina, B. E. Toki, M. Y. Torgov, B. A. Mendelsohn, C. G. Cervený, D. F. Chace, R. L. DeBlanc, R. P. Gearing, T. D. Bovee, C. B. Siegall, J. A. Francisco, A. F. Wahl, D. L. Meyer, P. D. Senter, Development of potent monoclonal antibody auristatin conjugates for cancer therapy. *Nat. Biotechnol.* **21**, 778–784 (2003).
27. A. Younes, U. Yasothan, P. Kirkpatrick, Brentuximab vedotin. *Nat. Rev. Drug Discov.* **11**, 19–20 (2012).
28. V. V. Leshchenko, Z. Hasanali, A. Stuart, S. Shimko, S. E. Spurgeon, S. Parekh, E. M. Epner, Combined epigenetic and immunotherapy for newly diagnosed mantle cell lymphoma: Correlative studies suggest the importance of enhanced ADCC, mechanisms of resistance and cyclin D1 nuclear localization genotype. 2013 Annual Meeting Abstracts, American Society of Hematology, New Orleans, LA, 7 to 10 December 2013, abstract 3063.
29. X. Sun, Z. S. Hasanali, A. Chen, D. Zhang, X. Liu, H. G. Wang, D. J. Feith, T. P. Loughran Jr., K. Xu, Suberoylanilide hydroxamic acid (SAHA) and cladribine synergistically induce apoptosis in NK-LGL leukaemia. *Br. J. Haematol.* **168**, 371–383 (2014).
30. K. Sharma, Z. Hasanali, S. Spurgeon, C. Okada, A. Stuart, S. Shimko, V. Leshchenko, S. Parekh, Y. Chen, M. Kirschbaum, E. M. Epner, Proceedings: AACR 104th Annual Meeting 2013, American Association for Cancer Research, Washington, DC, 6 to 10 April 2013, abstract LBA140.
31. B. Krawczyk, K. Rudnicka, K. Fabianowska-Majewska, The effects of nucleoside analogues on promoter methylation of selected tumor suppressor genes in MCF-7 and MDA-MB-231 breast cancer cell lines. *Nucleosides Nucleotides Nucleic Acids* **26**, 1043–1046 (2007).
32. M. Göttlicher, S. Minucci, P. Zhu, O. H. Krämer, A. Schimpf, S. Giavara, J. P. Sleeman, F. Lo Coco, C. Nervi, P. G. Pelicci, T. Heinzel, Valproic acid defines a novel class of HDAC inhibitors inducing differentiation of transformed cells. *EMBO J.* **20**, 6969–6978 (2001).
33. A. Cuker, A. J. Coles, H. Sullivan, E. Fox, M. Goldberg, P. Oyuela, A. Purvis, D. S. Beardsley, D. H. Margolin, A distinctive form of immune thrombocytopenia in a phase 2 study of alemtuzumab for the treatment of relapsing-remitting multiple sclerosis. *Blood* **118**, 6299–6305 (2011).
34. L. E. Ludlow, R. W. Johnstone, C. J. Clarke, The HIN-200 family: More than interferon-inducible genes? *Exp. Cell Res.* **308**, 1–17 (2005).
35. J. Tsukada, Y. Yoshida, Y. Kominato, P. E. Auron, The CCAAT/enhancer (C/EBP) family of basic-leucine zipper (bZIP) transcription factors is a multifaceted highly-regulated system for gene regulation. *Cytokine* **54**, 6–19 (2011).
36. J. Kim, H. Kim, Recruitment and biological consequences of histone modification of H3K27me3 and H3K9me3. *ILAR J.* **53**, 232–239 (2012).
37. E. Le Toriellec, G. Despouy, G. Pierron, N. Gaye, M. Joiner, D. Bellanger, A. Vincent-Salomon, M. H. Stern, Haploinsufficiency of *CDKN1B* contributes to leukemogenesis in T-cell prolymphocytic leukemia. *Blood* **111**, 2321–2328 (2008).
38. A. Yokohama, A. Saitoh, H. Nakahashi, T. Mitsui, H. Koiso, Y. Kim, H. Uchiyama, T. Saitoh, H. Handa, T. Jimbo, K. Murayama, T. Sakura, H. Murakami, M. Karasawa, Y. Nojima, N. Tsukamoto, *TCL1A* gene involvement in T-cell prolymphocytic leukemia in Japanese patients. *Int. J. Hematol.* **95**, 77–85 (2012).
39. P. J. De Schouwer, M. J. Dyer, V. B. Brito-Babapulle, E. Matutes, D. Catovsky, M. R. Yuille, T-cell prolymphocytic leukaemia: Antigen receptor gene rearrangement and a novel mode of *MTC1* B1 activation. *Br. J. Haematol.* **110**, 831–838 (2000).
40. J. Roos, I. Hennig, J. Schwaller, J. Zbären, R. Dummer, G. Burg, A. Tobler, L. Virgilio, C. M. Croce, M. F. Fey, B. Borisch, Expression of *TCL1* in hematologic disorders. *Pathobiology* **69**, 59–66 (2001).
41. Y. Pekarsky, C. Hallas, C. M. Croce, Targeting mature T cell leukemia: New understanding of molecular pathways. *Am. J. Pharmacogenomics* **3**, 31–36 (2003).
42. C. E. Dearden, A. Khot, M. Else, M. Hamblin, E. Grand, A. Roy, S. Hewamana, E. Matutes, D. Catovsky, Alemtuzumab therapy in T-cell prolymphocytic leukemia: Comparing efficacy in a series treated intravenously and a study piloting the subcutaneous route. *Blood* **118**, 5799–5802 (2011).
43. C. E. Dearden, E. Matutes, B. Cazin, G. E. Tjønnfjord, A. Parreira, B. Nomdedeu, P. Leoni, F. J. Clark, D. Radia, S. M. Rassam, T. Roques, N. Ketterer, V. Brito-Babapulle, M. J. Dyer, D. Catovsky, High remission rate in T-cell prolymphocytic leukemia with CAMPATH-1H. *Blood* **98**, 1721–1726 (2001).
44. Z. S. Hasanali, E. M. Epner, D. J. Feith, T. P. Loughran Jr., C. E. Sample, Vorinostat down-regulates CD30 and decreases brentuximab vedotin efficacy in human lymphocytes. *Mol. Cancer Ther.* **13**, 2784–2792 (2014).
45. R. A. Clark, R. Watanabe, J. E. Teague, C. Schlapbach, M. C. Tawa, N. Adams, A. A. Dorosario, K. S. Chaney, C. S. Cutler, N. R. Leboeuf, J. B. Carter, D. C. Fisher, T. S. Kupper, Skin effector memory T cells do not recirculate and provide immune protection in alemtuzumab-treated CTLCL patients. *Sci. Transl. Med.* **4**, 117ra117 (2012).
46. P. Gade, S. K. Roy, H. Li, S. C. Nallar, D. V. Kalvakolanu, Critical role for transcription factor C/EBP- β in regulating the expression of death-associated protein kinase 1. *Mol. Cell Biol.* **28**, 2528–2548 (2008).
47. H. Li, P. Gade, W. Xiao, D. V. Kalvakolanu, The interferon signaling network and transcription factor C/EBP- β . *Cell. Mol. Immunol.* **4**, 407–418 (2007).
48. E. Kiss-Toth, S. M. Bagstaff, H. Y. Sung, V. Jozsa, C. Dempsey, J. C. Caunt, K. M. Oxley, D. H. Wyllie, T. Polgar, M. Harte, L. A. O'Neill, E. E. Qvarnstrom, S. K. Dowder, Human tribbles, a protein family controlling mitogen-activated protein kinase cascades. *J. Biol. Chem.* **279**, 42703–42708 (2004).
49. H. Y. Sung, S. E. Francis, D. C. Crossman, E. Kiss-Toth, Regulation of expression and signalling modulator function of mammalian tribbles is cell-type specific. *Immunol. Lett.* **104**, 171–177 (2006).
50. M. Yamamoto, S. Uematsu, T. Okamoto, Y. Matsuura, S. Sato, H. Kumar, T. Satoh, T. Saitoh, K. Takeda, K. J. Ishii, O. Takeuchi, T. Kawaj, S. Akira, Enhanced TLR-mediated NF- κ B-dependent gene expression by Trib1 deficiency. *J. Exp. Med.* **204**, 2233–2239 (2007).

51. J. Xaus, M. Cardó, A. F. Valledor, C. Soler, J. Lloberas, A. Celada, Interferon γ induces the expression of p21^{waf-1} and arrests macrophage cell cycle, preventing induction of apoptosis. *Immunity* **11**, 103–113 (1999).
52. K. E. Mogensen, M. T. Bandu, Kinetic evidence for an activation step following binding of human interferon₂ to the membrane receptors of Daudi cells. *Eur. J. Biochem.* **134**, 355–364 (1983).
53. H. L. Rajala, S. Eldfors, H. Kuusanmaki, A. J. van Adrichem, T. Olson, S. Lagström, E. I. Andersson, A. Jerez, M. J. Clemente, Y. Yan, D. Zhang, A. Awwad, P. Ellonen, O. Kallioniemi, K. Wennerberg, K. Porkka, J. P. Maciejewski, T. P. Loughran Jr., C. Heckman, S. Mustjoki, Discovery of somatic STAT5b mutations in large granular lymphocytic leukemia. *Blood* **121**, 4541–4550 (2013).
54. O. R. Bandapalli, S. Schuessle, J. B. Kunz, T. Rausch, A. M. Stütz, N. Tal, I. Geron, N. Gershman, S. Izraeli, J. Eilers, N. Vaezipour, R. Kirschner-Schwabe, J. Hof, A. von Stackelberg, M. Schrappe, M. Stanulla, M. Zimmermann, R. Koehler, S. Avigad, R. Handgretinger, V. Frimantas, J. P. Bourquin, B. Bornhauser, J. O. Korbel, M. U. Muckenthaler, A. E. Kulozik, The activating STAT5B N642H mutation is a common abnormality in pediatric T-cell acute lymphoblastic leukemia and confers a higher risk of relapse. *Haematologica* **99**, e188–e192 (2014).
55. C. Kütçük, B. Jiang, X. Hu, W. Zhang, J. K. Chan, W. Xiao, N. Lack, C. Alkan, J. C. Williams, K. N. Avery, P. Kavak, A. Scuto, E. Sen, P. Gaulard, L. Staudt, J. Iqbal, A. Cornish, Q. Gong, Q. Yang, H. Sun, F. d'Amore, S. Leppä, W. Liu, K. Fu, L. de Leval, T. McKeithan, W. C. Chan, Activating mutations of STAT5B and STAT3 in lymphomas derived from $\gamma\delta$ -T or NK cells. *Nat. Commun.* **6**, 6025 (2015).
56. M. J. Kiel, T. Velusamy, D. Rolland, A. A. Sahasrabudhe, F. Chung, N. G. Bailey, A. Schrader, B. Li, J. Z. Li, A. B. Ozel, B. L. Betz, R. N. Miranda, L. J. Medeiros, L. Zhao, M. Herling, M. S. Lim, K. S. Elenitoba-Johnson, Integrated genomic sequencing reveals mutational landscape of T-cell prolymphocytic leukemia. *Blood* **124**, 1460–1472 (2014).
57. B. Khulan, R. F. Thompson, K. Ye, M. J. Fazzari, M. Suzuki, E. Stasiek, M. E. Figueroa, J. L. Glass, Q. Chen, C. Montagna, E. Hatchwell, R. R. Selzer, T. A. Richmond, R. D. Green, A. Melnick, J. M. Grealley, Comparative isoschizomer profiling of cytosine methylation: The HELP assay. *Genome Res.* **16**, 1046–1055 (2006).
58. R. Shaknovich, M. E. Figueroa, A. Melnick, HELP (Hpal tiny fragment enrichment by ligation-mediated PCR) assay for DNA methylation profiling of primary normal and malignant B lymphocytes. *Methods Mol. Biol.* **632**, 191–201 (2010).
59. V. V. Leshchenko, P. Y. Kuo, R. Shaknovich, D. T. Yang, T. Gellen, A. Petrich, Y. Yu, Y. Remache, M. A. Weniger, S. Rafiq, K. S. Suh, A. Goy, W. Wilson, A. Verma, I. Braunschweig, N. Muthusamy, B. S. Kahl, J. C. Byrd, A. Wiestner, A. Melnick, S. Parekh, Genomewide DNA methylation analysis reveals novel targets for drug development in mantle cell lymphoma. *Blood* **116**, 1025–1034 (2010).
60. R. F. Thompson, M. Suzuki, K. W. Lau, J. M. Grealley, A pipeline for the quantitative analysis of CG dinucleotide methylation using mass spectrometry. *Bioinformatics* **25**, 2164–2170 (2009).
61. E. Tuset, E. Matutes, V. Brito-Babapulle, R. Morilla, D. Catovsky, Immunophenotype changes and loss of CD52 expression in two patients with relapsed T-cell prolymphocytic leukaemia. *Leuk. Lymphoma* **42**, 1379–1383 (2001).
62. S. Göçmen, M. Kutlay, A. Eriççi, C. Atabey, O. Sayan, A. Haholu, Central nervous system involvement of T-cell prolymphocytic leukemia diagnosed with stereotactic brain biopsy: Case report. *Turkish J. Haematol.* **31**, 75–78 (2014).

Acknowledgments: We thank the Epigenomics and Genomics Cores of the Albert Einstein College of Medicine for expert technical assistance with HELP data. We thank R. Brucklacher and the Penn State Genomics Core along with T. Olson and X. Liu for microarray experimentation and analysis. We thank S. Kussick for CD52 and CD30 flow cytometry analyses, and M. Kester for discussion. **Funding:** This study was supported by the Chemotherapy Foundation to S.P., Gabrielle's Angel Foundation to S.P., Leukemia and Lymphoma Society Translational Research Project grant to S.P., Paul Calabresi Career Development Award K12-CA132783-01 to S.P., grants to E.M.E. from the Lymphoma Research Foundation and Tobacco Settlement funds of PA, and RO1-CA098472 from the National Cancer Institute to T.P.L. **Author contributions:** Z.S.H. and E.M.E. designed experiments, collected and interpreted data, and prepared the manuscript and clinical case studies; K.S. and B.S.S. helped with manuscript and clinical case study preparation; T.P.L. and S.P. were involved with data interpretation and manuscript preparation; A.S., S.S., M.V.S., V.V.L., and S.P. were involved with data collection and data interpretation; J.E. performed and interpreted tissue IHC. **Competing interests:** E.M.E. and K.S. are on the Speakers Bureau of Celgene; E.M.E. is on the Speakers Bureau of Seattle Genetics, Celgene, and Genzyme/Sanofi, and also serves as the Chief Scientific Officer of Sierra Epigenetics. The other authors declare that they have no competing interests. **Data and materials availability:** The microarray data for this study have been deposited in the Gene Expression Omnibus database (GSE67368).

Submitted 17 December 2014

Accepted 19 May 2015

Published 24 June 2015

10.1126/scitranslmed.aaa5079

Citation: Z. S. Hasanali, B. S. Saroya, A. Stuart, S. Shimko, J. Evans, M. V. Shah, K. Sharma, V. V. Leshchenko, S. Parekh, T. P. Loughran Jr., E. M. Epner, Epigenetic therapy overcomes treatment resistance in T cell prolymphocytic leukemia. *Sci. Transl. Med.* **7**, 293ra102 (2015).

Epigenetic therapy overcomes treatment resistance in T cell prolymphocytic leukemia

Zainul S. Hasanali, Bikramajit Singh Saroya, August Stuart, Sara Shimko, Juanita Evans, Mithun Vinod Shah, Kamal Sharma, Violetta V. Leshchenko, Samir Parekh, Thomas P. Loughran, Jr. and Elliot M. Epner

Sci Transl Med 7, 293ra102293ra102.
DOI: 10.1126/scitranslmed.aaa5079

A second chance for leukemia therapy

T cell prolymphocytic leukemia (T-PLL) is a rare and aggressive type of leukemia, which is usually difficult to treat. Alemtuzumab, a monoclonal anti-CD52 antibody, is currently used to treat this disease, but patients quickly develop resistance to alemtuzumab or do not respond to it altogether. Now, Hasanali *et al.* show that epigenetic therapy can help overcome drug resistance in T-PLL patients. In addition, the epigenetic drugs frequently up-regulated CD30 on the surface of leukemia cells, which allowed subsequent successful treatment with brentuximab vedotin, an antibody-drug conjugate targeting CD30. The findings suggest a new treatment regimen for this challenging disease and demonstrate a potential approach to successfully combining epigenetic and immunotherapy.

ARTICLE TOOLS

<http://stm.sciencemag.org/content/7/293/293ra102>

SUPPLEMENTARY MATERIALS

<http://stm.sciencemag.org/content/suppl/2015/06/22/7.293.293ra102.DC1>

RELATED CONTENT

<http://stm.sciencemag.org/content/scitransmed/6/229/229ra41.full>
<http://stm.sciencemag.org/content/scitransmed/5/177/177ra38.full>
<http://stm.sciencemag.org/content/scitransmed/5/169/169ra10.full>
<http://stm.sciencemag.org/content/scitransmed/4/156/156ra140.full>
<http://stm.sciencemag.org/content/scitransmed/4/134/134ra63.full>
<http://stm.sciencemag.org/content/scitransmed/7/306/306fs38.full>
<http://stm.sciencemag.org/content/scitransmed/8/339/339ra69.full>
<http://stm.sciencemag.org/content/scitransmed/8/339/339ra70.full>

REFERENCES

This article cites 60 articles, 20 of which you can access for free
<http://stm.sciencemag.org/content/7/293/293ra102#BIBL>

PERMISSIONS

<http://www.sciencemag.org/help/reprints-and-permissions>

Use of this article is subject to the [Terms of Service](#)

Science Translational Medicine (ISSN 1946-6242) is published by the American Association for the Advancement of Science, 1200 New York Avenue NW, Washington, DC 20005. The title *Science Translational Medicine* is a registered trademark of AAAS.

Copyright © 2015, American Association for the Advancement of Science